Available online at www.sciencedirect.com

SciVerse ScienceDirect

Ceramics International 38 (2012) 6423–6429

CERAMICS INTERNATIONAL

www.elsevier.com/locate/ceramint

Study of the high temperature oxidation performance of Thermal Barrier Coatings with HVOF sprayed bond coat and incorporating a PVD ceramic interlayer

C.R.C. Lima[a,*], N. Cinca[b], J.M. Guilemany[b]

[a] *Methodist University of Piracicaba, Rodovia Santa Bárbara-Iracemápolis, Km 1 Santa Bárbara d'Oeste, SP 13450-000, Brazil*
[b] *Thermal Spray Center (CPT), University of Barcelona C/Marti y Franqués, 1, Barcelona 08028, Spain*

Received 21 March 2012; received in revised form 4 May 2012; accepted 5 May 2012
Available online 17 May 2012

Abstract

The performance of an intermediate Cr_3C_2 ceramic layer applied by PVD between the bond coat and the ceramic top coat in a TBC system was evaluated. The thickness of the transitional layer was kept around 1–2 μm. Two substrate materials and two distinct bond coats were combined in the tests. High Velocity Oxygen Fuel (HVOF) and Atmospheric Plasma Spraying (APS) were used respectively for bond coat and top coat deposition. Isothermal oxidation tests were performed at 1000 °C in static air atmosphere. Thermal grown oxide (TGO) was measured and correlated to the exposition times. Results are discussed in terms of the TGO growth rate and changes in residual stresses. The results suggest an improvement in the oxidation resistance of the bond coat because of the presence of the intermediate layer.

Keywords: Thermal Barrier Coatings; Oxidation; TGO; Intermediate layers

1. Introduction

Thermal Barrier Coatings (TBC) are widely used to protect gas turbines as well as diesel engine parts from severe working conditions in elevated temperature environments [1–3]. A TBC system typically consists of a superalloy substrate, a metallic bond coat and a ceramic top coat. Some studies include the thermally grown oxide layer (TGO) as a part of the system despite of it being a reaction product that forms because of bond coat oxidation as oxygen moves through the interconnected pores of the ceramic top coat in cyclic service heating [4,5]. Zirconia has been stated as the elected ceramic material, mainly partially stabilized Zirconia with addition of 7%–8% Yttria in solid solution (ZrO_2 7%–8%wt Y_2O_3) [5–8]. The ceramic layer is normally applied by Atmospheric Plasma Spray (APS) or Electron Bean assisted Physical Vapor Deposition (EB-PVD) [3,8]. Investigation on HVOF application of ceramic materials for TBC has also been done [9]. The bond coat usually consists of a MCrAlY alloy, where M stands for Ni, Fe, Co or some combination of them. Some alloys also include other materials like Y, Hf, Ta or Re [10,11]. The bond coat has the function of protecting the substrate from oxidation and hot corrosion, forming an oxide layer at the interface that protects and helps in the anchorage of the ceramic layer, with a coefficient of thermal expansion (CTE) between that of the metallic substrate and that of the ceramic. The usual methods for applying metallic bond coats are Air Plasma Spraying (APS), the lowest cost alternative, Vacuum Plasma Spraying (VPS) or Low Pressure Plasma Spraying (LPPS) [3,12]. HVOF spraying has been more recently used as an alternative deposition method because of its low cost and high quality deposits, which have oxidation rates at high temperature at the same level or even lower than those of similar VPS or LPPS coatings [8,10,11,13,14]. With this low oxidation perspective, some studies have also been done by using cold sprayed metallic bond coats [15,16].

---

[*] Corresponding author. Tel.: +55 19 31241785; fax: +55 19 34551361.
E-mail address: crclima@unimep.br (C.R.C. Lima).

0272-8842/$36.00 © 2012 Elsevier Ltd and Techna Group S.r.l. All rights reserved.
http://dx.doi.org/10.1016/j.ceramint.2012.05.016

Events that result in the degradation of a TBC in service are bond coat delamination caused by the infiltration of gases at high temperature because of ceramic layer permeability, the differences of thermal expansion coefficient between metallic and ceramic layers, the growth of an oxide layer onto the bond coat (Thermally grown oxide—TGO) and Al diffusion from the substrate. The differences of thermal expansion coefficients between metallic bond coat and ceramic top coat cause residual stresses. Such residual stresses as well as the stresses caused by bond coat oxidation and consequent increase in the TGO layer lead to ceramic debonding and subsequent failure of the thermal barrier system [17,18]. The growth rate and adherence of the TGO is one of the most relevant factors determining TBC lifetime and very small amounts of reactive elements would affect TGO growth and adherence [12,19].

Extensive investigation has been carried out with the main objective of improving the characteristics of adherence and oxidation resistance at high temperatures (above 1000 °C) of the TBCs. The use of graded structures or Functionally Graded Materials—FGM [20,21], nanostructured materials [22,23], diffusion barrier layers [24] and intermediate layers [25] with specific functions as well as addition of dopants to the bond coat have been explored [11]. Recent studies deal with in situ forming of an amorphous TGO during spark plasma sintering fabrication of TBC systems [26]. In this work the use of an intermediate layer between the bond coat and the ceramic top coat is investigated. The intermediate layer is a highly corrosion resistant Cr_3C_2 applied by Physical Vapor Deposition (PVD).

2. Experimental procedure

The TBC system proposed is schematically shown in Fig. 1. Two types of substrates and two distinct bond coats were combined in the tests. Cylindrical (50 mm diameter and 5 mm thickness) substrates of UNS G41350 steel and IN 718 Ni based superalloy were used for sample characterization or oxidation tests. Two types of materials were alternatively used as bond coats: CoNiCrAlY (Amdry 9951-Sulzer Metco) and NiCoCrAlTaY (Amdry 997-Sulzer Metco).

The ceramic top coat used was ZrO_2-8%wt Y_2O_3 (203-NS-Sulzer Metco) for all the applied systems. The morphology of the metallic and ceramic powders used is shown in Fig. 2. The two bond coat powder materials presented a difference in average grain size of about 25%. Despite the coarser grain size of NiCoCrAlTaY powder (Amdry 997), both bond coat powders have a spherical morphology. Ceramic powder also presents a spherical morphology but much higher grain size dispersion. The intermediate layer was a Cr_3C_2 applied by Physical Vapor Deposition (PVD). The main characteristics and composition of the powders are shown in Table 1.

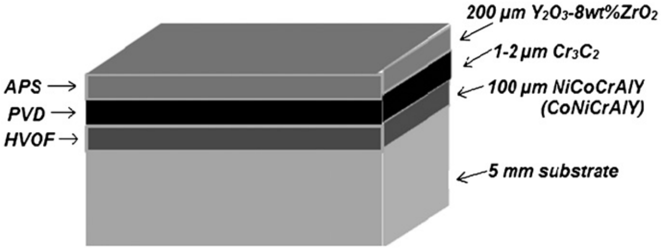

Fig. 1. Scheme of the proposed TBC systems.

Just before spraying, the substrates were degreased with acetone and grit blasted with white corundum at 5.6 bar, 45° blasting incidence angle and a blasting distance of 250 mm. The grit blasted substrates had a mean roughness (*Ra*) of 5 μm. Samples were placed in a circular sample holder and were simultaneously sprayed for every material with a rotational speed of 500 mm s^{-1} in the substrate surface. Air jet was used as cooling media for ceramic spraying directed to sample back side. The matrix of sprayed TBC systems is shown in Table 2.

The bond coats were produced by using a High Velocity Oxygen Fuel (HVOF) spraying system Model DJ-2600/2700 (Sulzer Metco Inc., Westbury, NY, USA). A F4-MB plasma spray gun (Plasma Technik, Sulzer Metco, Westbury, USA) was used to apply the ceramic top coats. The thermal spraying parameters used for metallic and ceramic coatings application are shown in Table 3.

Laser Scattering (Microtrac SRA150), Scanning Electron Microscopy (SEM) and flow rate test (ASTM B-213-90) were

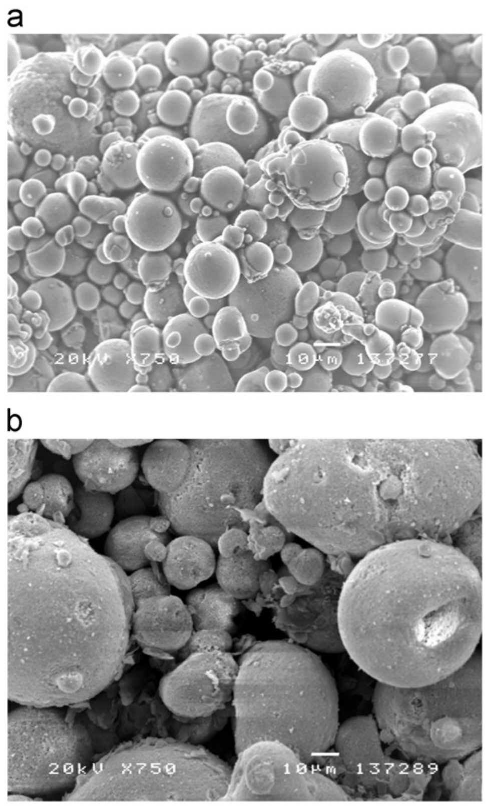

Fig. 2. Spherical morphology of (a) metallic NiCoCrAlTaY and (b) ceramic $ZrO_2Y_2O_3$ powders.

Table 1
Characteristics and composition of the metallic and ceramic used powders.

Powder	Composition (wt%)								Grain size (μm)		Morphology
	Co	Ni	Cr	Al	Ta	Y	ZrO_2	Y_2O_3	$\overline{x}$	σ	
Amdry 9951	38.5	32	21	8	–	0.5	–	–	21.5	9.2	Spherical
Amdry 997	23	43.9	20	8.5	4	0.6	–	–	27.0	11.6	Spherical
203-NS	–	–	–	–	–	–	92	8	65.3	30.2	Spherical

Table 2
Arrangement of the sprayed TBC systems.

Substrate	Bond coat 1: CoNiCrAlY	Bond coat 2: NiCoCrAlTaY
UNS G41350	System S1	System S2
In 718	System S3	System S4

used for powder particle size distribution and for general characterization. XRD (Siemens D-500, Cu $K\alpha = 1.5418$ Å, 40 KV, 30 mA) was applied to reveal phase content of the starting powder. Samples characterization included cross-sectional Optical Microscopy (Olympus BH-2-UMA) and Scanning Electron Microscopy (JEOL—JSM- 5310) images, as well as phase analysis by Energy Dispersive Spectroscopy—EDS (Quantum, Kevex). Coating surface roughness was measured using a Surftest 301 (Mitutoyo). Values quoted for both microhardness and roughness are an average of 20 measurements for each coating. For the intermediate layer application, Cr_3C_2 was chosen because of its high corrosion resistance, thermal stability until approximately 900 °C and a Coefficient of Thermal Expansion (CTE) of $10.3 \times 10^{-6}\,°C^{-1}$, very close to those of bond coats ($14 \times 10^{-6}\,°C^{-1}$) and ceramic top coat ($10.6 \times 10^{-6}\,°C^{-1}$). The CTE of chromium carbide is also close to that of steel, reducing the mechanical stress buildup at the layer boundary.

PVD was used to apply the thin intermediate layer. An anchorage layer of CrN was used for Cr_3C_2 application. The thickness was kept around 1–2 μm. The process parameters used are shown in Table 3 and Table 4 respectively for thermal spray and PVD.

Isothermal oxidation tests were performed at 1000 °C in static air atmosphere. Samples were protected from the aggressive environment with a cement material, leaving only the coating surface exposed to the environment. Sets of samples were exposed for 12, 24, 48 and 96 h. After cooling in ambient air the samples were metalographically prepared to be observed by SEM. The thermal grown oxide (TGO) layer was then measured and correlated to exposition times.

3. Results

3.1. Structural characterization

A representative image of the TBC system S1 is shown in Fig. 3. The general microstructure of the coatings was practically identical for the two bond coat materials. A typical image of the intermediate Cr_3C_2 PVD layer obtained onto the CoNiCrAlY bond coat before the application of the ceramic top coat can be observed in Fig. 4. An adherent layer was formed with a little intermittence which could have been caused by process parameters adjustment. After top coat deposition the PVD intermediate layer was more difficult to identify by SEM analysis. EDS was more frequently applied to help in the analysis. PVD layer has still shown some intermittence which can be observed in Fig. 5 that can be related to the inherent roughness profile of the bond coat measured around 6.5 μm in the "as-sprayed" condition.

The typical X-ray diffraction of the top surface of a coated specimen and of the two bond coatings used is presented in Fig. 6. The bond coat of NiCoCrAlTaY shows higher presence of Cr that was also detected in the as-sprayed coating (Fig. 5) in the bond coat/intermediate layer interface by EDS.

3.2. Isothermal oxidation results

The results of high temperature isothermal oxidation tests are graphically shown in Fig. 7. The coating systems have shown a relatively similar TGO thickness after the first 12 and 24 h of isothermal exposition. Some increase in the thickness of TGO can be observed after 48 and after 96 h of testing, i.e, a factor of 1.5 thickness growth after 48 h and about 2 after 96 h.

However, it should be noted that the systems S1 and S3, having the PVD intermediate layer onto a CoNiCrAlY bond coat, show slightly smaller values of TGO thickness compared to S2 and S4 that has a NiCoCrAlTaY bond coat. This trend could be related to the higher Ni content in the coating, considering the original composition of the two bond coat materials. Nickel enables the creation of phases of high melting temperature and high oxidation resistance like β-NiAl phase [27]. As cobalt easily substitutes nickel atoms and improves oxidation resistance the higher content of the pair Ni–Co in the CoNiCrAlY bond coat could lead to a lower oxide formation.

SEM cross sectional micrographs of representative tested samples with the intermediate layer are shown in Fig. 8 for 12, 24, 48 and 96 h of test.

Table 3
General thermal spraying parameters.

HVOF	Oxygen		Propylene		Air		Powder feed rate (g/min)	Stand off distance (mm)
	Pressure (bar)	Flow rate (SLPM)	Pressure (bar)	Flow rate (SLPM)	Pressure (bar)	Flow rate (SLPM)		
CoNiCrAlY	10.3	139	6.9	89	7.2	384	38	250
NiCoCrAlTaY	10.3	139	6.9	89	7.2	384	38	250
APS	Ar flow rate (l/min)		H_2 Flow Rate (l/min)		Amperage (A)	Voltage (V)	Layers	Stand off distance (mm)
ZrO_2–8%Y_2O_3	40		12		630	68	20	120

Table 4
PVD process parameters.

	Time (min)	Temp. (°C)	Gas	Gas pressure (mbar)	Caudal (sccm)	Voltage (V)	Amperage (A)
Heating	2		Ar	1.5×10^{-3}	100	1000	60
Coating CrN	5	350	N_2	6×10^{-3}	300	150	60
Coating Cr_3C_2	30	–	C_2H_2	6×10^{-3}	30	180	80
Initial vacuum: 8×10^{-5} mbar				Number of Cr cathodes: 02			

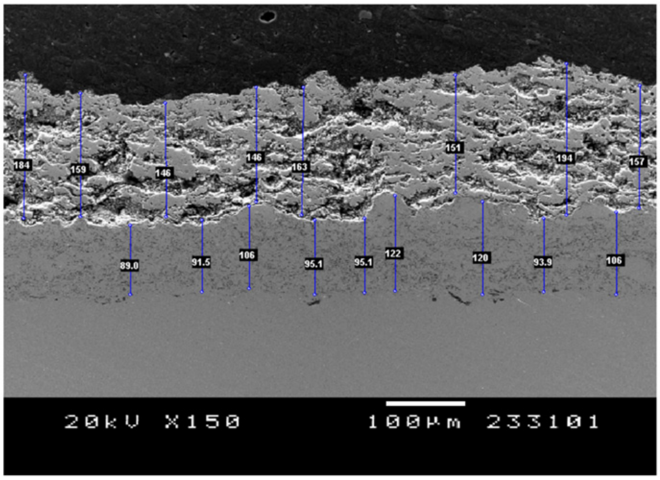

Fig. 3. SEM cross section of the TBC system S1 with a CoNiCrAlY bond coat applied onto UNS G41350 steel. The thicknesses of the metallic and ceramic layers are indicated by the arrows showing a larger variation in the bond coat due to intrinsic roughness.

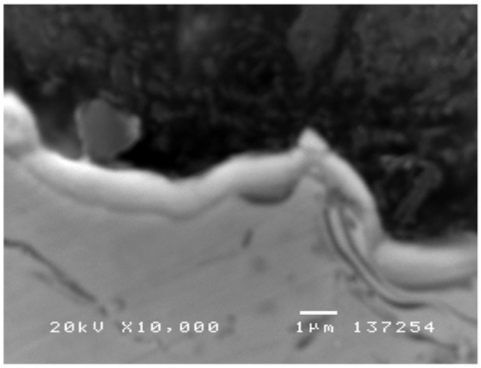

Fig. 4. Cross section back scattered SEM image of the Cr_3C_2 intermediate layer applied by PVD onto a NiCoCrAlTaY metallic bond coat. A very regular and smooth layer can be observed.

4. Discussion

4.1. *TGO growth rate*

From the first results at 12 h of testing to 24 h the TGO thickness did not considerably increase. After 96 h of oxidation test the thickness of the TGO layer increased about 2 μm from the measured thickness after 24 h of testing reaching a maximum of 4.2 μm and it is basically formed of Al_2O_3 as expected. Alumina is the preferred thermally grown oxide because of its low oxygen diffusivity and superior adherence. The rate of TGO growth is low compared to previous works. Limarga [21] working with YSZ-NiCoCrAlY system obtained a 6 μm thick TGO after 18 h of isothermal exposition at 1050 °C and a maximum of 8 μm thick TGO after 96 h of testing, two times thicker than the results of this work. In a research developing a YSZ-MCrAlY with high oxidation resistance, Matsumoto [28] obtained a 6 μm thick TGO after 10 h of isothermal exposition at 1200 °C and 9 μm thick after 50 h of testing.

Although the work arrangement with no further thermal cycling testing do not allow to state with certainty, the experimental results suggest that a very thin layer of Cr_3C_2 applied on the metallic bond coat before ZrO_2 top coat application can improve oxidation resistance by retarding or even suppressing some oxidation reactions because of low oxygen diffusivity and phase stability of Cr_3C_2 scale. Also Cr_3C_2 chemical reactions may be beneficial because of the high temperature oxidation resistance nature of the Cr_2O_3 oxide eventually formed and consequent reduction of the indispensable amount of aluminum which is necessary to create the α-Al_2O_3 oxide typical of TGO. Based on the measurement of the thickness of TGO formed at the interface it is believed that Cr_3C_2 material is effective in reducing the oxidation rate of the TBC system.

The TGO region of the TBC system S3 after 24 h of isothermal oxidation is shown in Fig. 9. The presence of Cr_3C_2 and Al rich oxides can be observed. At the surface of the Al_2O_3 layer (TGO) other oxides and spinels containing Ni, Co and Cr were detected.

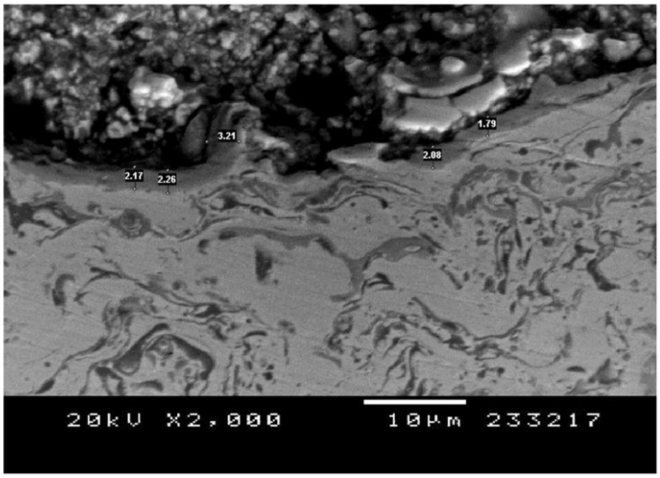

Fig. 5. Cross section back scattered SEM image of the TBC system S2 after 24 h of isothermal oxidation showing the Cr_3C_2 intermediate layer, NiCoCrAlTaY metallic bond coat and YSZ top coat. The thickness of the PVD layer is around 2 μm as indicated by the measurement arrows.

4.2. The role of residual stresses

As a consequence of the oxidation rate reduction, large residual stress associated with the formation of TGO at bond cot/top coat interface could be minimized. Residual stresses in coatings are the subject of several investigations and are still not fully understood given that the mechanisms of formation are complex and the stress state varies with location, resulting in a stress distribution within the coating that causes spallation of the ceramic top coat. Residual stresses occur from a combination of macro and micro effects that include CTE mismatch between the coating and substrate and the differential thermal expansion coefficients between different phases present in the coating. The stress close to the bond coat is higher than close to the ceramic. The stress at thickness imperfections in the TGO is smaller than in the regular TGO close to the bond coat [29]. With the application of an intermediate layer, stress distribution would change in a certain way mainly because of modifications on the surface imperfections in that region and also by changing oxidation kinetics.

Further evaluation with deep chemical analysis is intended in order to further study the complex oxidation products that are formed in the TGO region with the intermediate layer and the resulting residual stress distribution.

5. Conclusions

An intermediate Cr_3C_2 layer was applied by PVD in Thermal Barrier Coatings systems composed of distinct

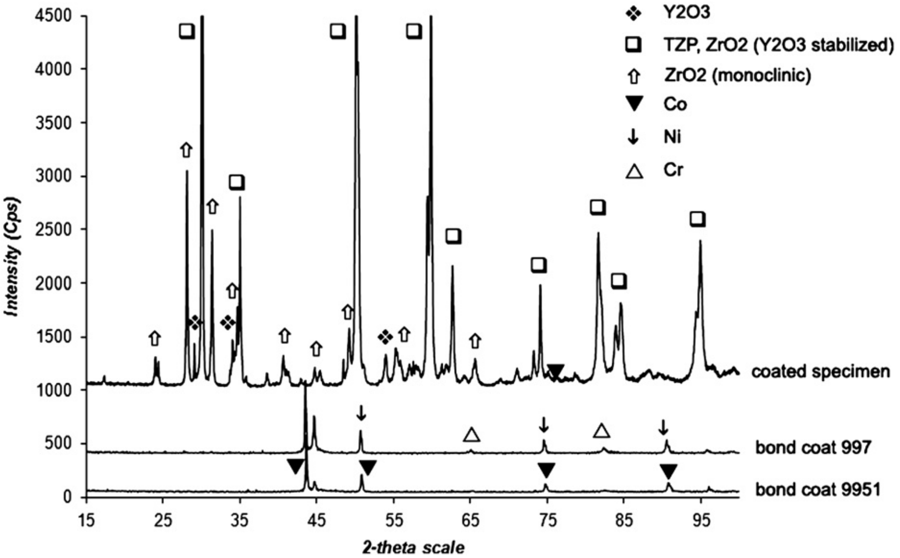

Fig. 6. X-ray diffraction of the ceramic top coating, the CoNiCrAlY (9951) and NiCoCrAlTaY (997) bond coatings.

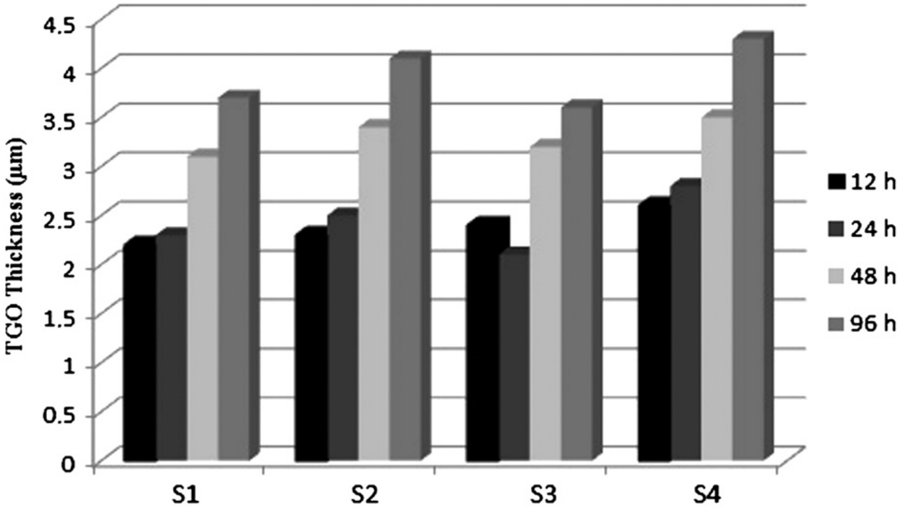

Fig. 7. TGO thickness for the different TBC systems after 12, 24, 48 and 96 h of isothermal oxidation testing performed at 1000 °C in static air atmosphere. Systems S1 and S3 have a CoNiCrAlY bond coat; S2 and S4 have a NiCoCrAlTaY bond coat.

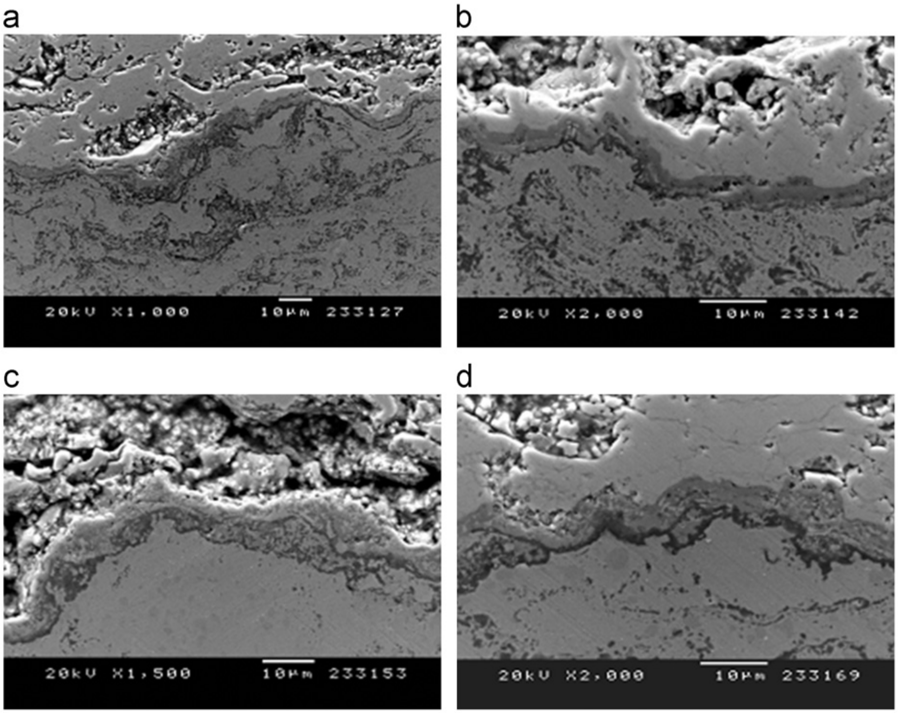

Fig. 8. SEM cross section of a S1 system (CoNiCrAlY bond coat onto UNS G41350 steel) sample with the Cr_3C_2 intermediate layer showing the TGO layer after (a) 12 h, (b) 24 h, (c) 48 h and (d) 96 h of isothermal oxidation performed at 1000 °C in static air atmosphere.

bond coats applied by HVOF spraying. The samples were evaluated by isothermal oxidation tests and microstructural observation by means of Scanning Electron and Optical Microscopy.

The results can be summarized as follows:

(1) The distinct materials applied as bond coats, mainly differing in the chemical Co and Ni composition and powder grain size, have shown similar behavior in oxidation tests.

(2) The use of the intermediate layer suggests an improvement in the oxidation resistance of the bond coat since a thinner TGO forms in the system showing a low oxidation rate.

(3) Some modification in residual stresses may also be suggested because of the presence of an intermediate layer that changes stress distribution mainly because of corrections on the surface imperfections in that region and also by changing oxidation kinetics.

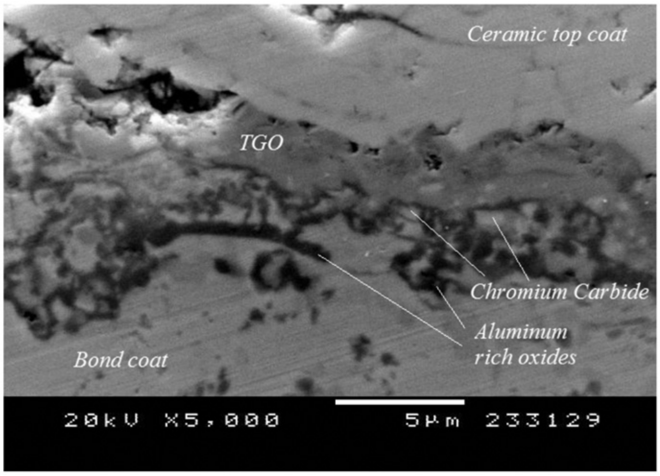

Fig. 9. SEM cross section of TBC system S3 (CoNiCrAlY bond coat onto IN 718) sample after 24 h of isothermal oxidation performed at 1000 °C in static air atmosphere showing the TGO layer, Al rich oxides and the evidence of the presence of Cr_3C_2 intermediate layer.

Acknowledgments

The authors would like to thank TTCarreras Group from Spain for PVD application and the Project 2009 no. SGR00310 from the Generalitat de Catalunya. Financial support from the CNPq-Brazil is also acknowledged.

References

[1] R.N. Katz, Thermal barrier coatings beat the heat, Ceram. Ind. 151 (4) (2001) 22–23.

[2] J.P. Huchin, The place of thermal spraying in industry today and the prospects for the future, in: C. Coddet (Ed.), Thermal Spray: Meeting the Challenges of the 21st Century, vol. 2, ASM International, Materials Park, Ohio, USA, 1998, pp. 925–931.

[3] A.G. Evans, D.R. Mumm, J.W. Hutchinson, G.H. Meier, F.S. Pettit, Mechanisms controlling the durability of thermal barrier coatings, Progress in Materials Science 46 (2001) 505–553.

[4] N.P. Padture, M. Gell, E.H. Jordan, Thermal barrier coatings for gas-turbine engine applications, Science 296 (2002) 280–284.

[5] M.D. Hill, Creating an effective barrier, Industrial Ceramics 153 (10) (2003) 17–19.

[6] D. Stover, G. Pracht, H. Lehmann, M. Dietrich, J.E. Doring, R. Vaben, New material concepts for the next generation of plasma-sprayed thermal barrier coatings, in: C. Moreau, B. Marple (Eds.), Thermal Spray2003: Advancing the Science and Applying the Technology, (Ed.), ASM International, Materials Park, Ohio, USA, 2003, pp. 1455–1462.

[7] H. Van Esch, J. DeBarro, Coating selection critical to turbine performance, Power Engineering 102 (7) (1998) 44–47.

[8] Y. Itoh, M. Saitoh, M. Tamura, Characteristics of MCrAlY coatings sprayed by high velocity oxygen-fuel spraying system, Journal of Engineering for Gas Turbines and Power 122 (2000) 43–49.

[9] T.A. Dobbins, R. Knight, M.J. Mayo, HVOF thermal spray deposited Y_2O_3-stabilized ZrO_2 coatings for thermal barrier applications, Journal of Thermal Spray Technology 12 (2) (2003) 214–225.

[10] P. Vuoristo, S. Ahmaniemi, S. Tuurna, T. Mantyla, E. Cordano, F. Fignino, G.C. Gualco, Development of HVOF sprayed NiCoCrAlYRe coatings for use as bond coats of plasma sprayed thermal barrier coatings, in: Proceedings of the ITSC 2002—International Thermal Spray Conference and Exposition, vol. 1, Essen, Germany, ASM-International/DVS, 2002, pp. 470–475.

[11] W.O. Soboyejo, P. Mensah, R. Diwan, J. Crowe, S. Akwaboa, High temperature oxidation interfacial growth kinetics in YSZ thermal barrier coatings with bond coatings of NiCoCrAlY with 0.25% Hf, Materials Science and Engineering A: Structural Materials 528 (2011) 2223–2230.

[12] M. Subanovic, P. Song, E. Wessel, R. Vassen, D. Naumenko, L. Singheiser, W.J. Quadakkers, Effect of exposure conditions on the oxidation of MCrAlY-bondcoats and lifetime of thermal barrier coatings, Surface and Coatings Technology 204 (2009) 820–823.

[13] B.A. Pint, M.A. Bestor, J.A. Haynes, Cyclic oxidation behavior of HVOF bond coatings deposited on La- and Y-doped superalloys, Surface and Coatings Technology 206 (2011) 1600–1604.

[14] K.G. Schmitt-Thomas, H. Haindl, D. Fu, Modifications of thermal barrier coatings (TBCs), Surface and Coatings Technology 94–95 (1997) 149–154.

[15] P. Richer, M. Yandouzi, L. Beauvais, B. Jodoin, Oxidation behaviour of CoNiCrAlY bond coats produced by plasma, HVOF and cold gas dynamic spraying, Surface and Coatings Technology 204 (2010) 3962–3974.

[16] A. Manap, D. Seo, K. Ogawa, Characterization of thermally grown oxide on cold sprayed CoNiCrAlY bond coat in thermal barrier coating, Materials Science Forum 696 (2011) 324–329.

[17] P. Scardi, M. Leoni, L. Bertini, L. Bertamini, F. Cernuschi, Strain gradients in plasma-sprayed zirconia thermal barrier coatings, Surface and Coatings Technology 108–109 (1998) 93–98.

[18] P. Scardi, M. Leoni, L. Bertamini, M. Marchese, Residual stresses in plasma sprayed Y_2O_3-PSZ coatings on piston heads, Surface and Coatings Technology (1996) 109–11586-87 (1996) 109–115.

[19] A. Bennett, F.C. Roriz, A.B. Thakker, Surface and Coatings Technology 32 (1987) 359.

[20] S. Rangaraji, K. Kokini, Interface thermal fracture in functionally graded zirconia-mullite-bond coat alloy thermal barrier coating, Acta Materialia 51 (2003) 251–267.

[21] A.M. Limarga, S. Widjaja, T.H. Yip, Mechanical properties and oxidation resistance of plasma-sprayed multilayered Al_2O_3/ZrO_2 thermal barrier coatings, Surface and Coatings Technology 197 (2005) 93–102.

[22] R.S. Lima, A. Kucuk, C.C. Berndt, Integrity of nanostructured partially stabilized zirconia after plasma spray processing, Journal of Materials Science and Technology A313 (2001) 75–82.

[23] Y. Zeng, S.W. Lee, L. Gao, C.X. Ding, Atmospheric plasma sprayed coatings of nanostructures zirconia, Journal of the European Ceramic Society 22 (2002) 347–351.

[24] M. Matsumoto, H. Takayama, D. Yokoe, K. Mukai, H. Matsubara, Y. Kagiya, Y. Sugita, Scripta Materialia 54 (2006) 2035–2039.

[25] C.R.C. Lima, J.M. Guilemany, Functional intermediate layers for the improvement of Thermal Barrier Coatings performance, in: Proceedings of the Materials Science and Technology Conference and Exhibition, MS and T'07—"Exploring Structure, Processing, and Applications Across Multiple Materials Systems", vol. 4, 2007, pp. 2204–2211.

[26] M. Boidot, S. Selezneff, D. Monceau, D. Oquab, C. Estournès, Proto-TGO formation in TBC systems fabricated by spark plasma sintering, Surface and Coatings Technology 205 (2010) 1245–1249.

[27] G. Moskal, Thermal barrier coatings: characteristics of microstructure and properties, generation and directions of development of bond, Journal of Achievements in Materials and Manufacturing Engineering 37-2 (2009) 323–331.

[28] M. Matsumoto, Development of Plasma Sprayed Thermal Barrier Coatings with low thermal conductivity and high oxidation resistance, Journal of the Ceramic Society of Japan 115 (2) (2007) 118–123.

[29] T. Tomimatsu, S. Zhu, Y. Kagawa, Effect of thermal exposure on stress distribution in TGO layer of EB-PVD TBC, Acta Materialia 51 (2003) 2397–2405.